Journal of Microelectronics and Electronic Packaging (2014) **11**, 30-35

ISSN: 1551-4897

Mechanical Stress Analyses of Packaged Pressure Sensors for Very High Temperatures

Roderich Zeiser,* Suleman Ayub, Jochen Hempel, Michael Berndt, and Juergen Wilde

***Abstract*—Methods for investigations of stresses specialized for devices operating up to 500°C are presented in this study. Resistive pressure sensors and test chips with microstrain (μ-strain) gauges are processed in thin film technology. The sensor structure was a Wheatstone bridge on a silicon membrane with platinum resistors. The μ-strain gauges were characterized with tensile tests in combination with optical strain measurements. A gauge factor of 3.6 was measured at room temperature. After characterization as bare dice, the chips were mounted with a borosilicate glass solder on two ceramic substrates, AlN and Si_3N_4. We generated a FE model of the sensor assemblies including temperature-dependent material properties. The distribution of mechanical strains and stresses in the sensor was analyzed. The chip warpage dependent on temperature up to 500°C was obtained from FE simulations and compared with high-precision 3D deformation measurements. Deformation results from digital image correlation (DIC) verified the utilized FE model. The correlation of experimental results for the chip warpage exhibited good agreement with the numerical results obtained from FEM. The chip deflection from the center to the edges in the out-of-plane direction on AlN was 4.5 μm; on Si_3N_4 a concave warpage of 3 μm at 25°C was found. Temperature-induced deformations of the sensor chip in the range of micrometers were recorded up to 500°C. The output signal of the pressure sensors is strongly affected by superimposed strains based on the sensor assembly. The bridge voltage increased by 40% after the glass solder process on AlN and by 34% for devices on Si_3N_4. The analysis of the μ-strain gauges showed compressive strains in the sensor membrane of −1.39% on average for assemblies on AlN and of −0.168% for glass soldered chips on Si_3N_4. The FEM simulations revealed an average in-plane stress in the sensor membrane of −45 MPa for chips on AlN and −20 MPa for Si_3N_4 substrates. The compressive strains in the membrane obtained by FEM were verified by the μ-strain gauge measurements. A higher strain and stress gradient in the membrane of devices on AlN was found with FEM, which is consistent with the higher signal offset of assembled pressure sensors that was measured in this study.**

***Keywords*—Digital image correlation (DIC), high temperature, packaging stress, pressure sensor, strain gauges**

Received on September 25, 2013; revision received on November 11, 2013; accepted on November 12, 2013

The original manuscript version of this paper was presented at IMAPS 46th International Symposium on Microelectronics (IMAPS 2013), September 30-October 3, 2013, Orlando, FL, USA.

University of Freiburg, IMTEK, Georges-Koehler-Allee 103, 79110 Freiburg, Germany

*Corresponding author; email: roderich.zeiser@imtek.uni-freiburg.de

Introduction

In the fields of industrial facilities, aircraft, and automotive applications, it is necessary to collect data about the condition of machines, processes, or the surrounding environment. Sensors that can operate in harsh environments at high temperatures (HT) around 500°C can increase the effectiveness of machines such as motors, turbines, or chemical reactors. Electronic devices that can survive and operate at temperatures above 500°C are rare. In the past, several approaches with silicon carbide and platinum-based sensor structures were made to achieve the advantages of MEMS-based sensors under these extreme harsh operating conditions [1, 2]. Despite the low number of high-temperature stable sensor systems, there are various applications where such sensors can be applied. The reliability of the already existing HT sensor elements and their assembly and packaging technologies still needs to be developed and improved. Only a few published studies address the reliability of high-temperature packaging technology [3]. We demonstrate several approaches to analyze the mechanical stresses in sensors that are suitable to operate up to 500°C. Stress analyses of HT sensors and their packages will improve their reliability and contribute to the development of MEMS devices in the field of extreme harsh conditions.

Theory

In this study, platinum thin films act as strain gauges on membranes for pressure sensors. The sensor membrane deflects due to a pressure applied to the sensor element. This deflection leads to strains in the membrane surface that can be detected by resistive structures.

In eq. (1), the change of the initial resistance R_0 of a metallic film due to the applied strain ε is given. The gauge factor, k, can be computed with eq. (1).

$$\Delta R = R_0 \cdot k \cdot \varepsilon = R_0 \cdot k \cdot \frac{\Delta l}{l_0}. \quad (1)$$

In eq. (2), ρ is the resistivity, ν is Poisson's ratio, and ε is the applied strain.

$$k \approx (1 + 2\nu) + \frac{d\rho}{\rho \cdot d\varepsilon}. \quad (2)$$

The first term of eq. (2) defines the geometric effect of the change in resistance; and the second term describes the

doi:10.4071/imaps.399

physical effect of the change in resistivity, which is negligible for most metals [4].

Sensors and Packaging Technology

A. Pressure Sensor and Strain Gauges

The sensors are processed in thin film technology with 500 nm thick platinum films on oxidized silicon wafers. KOH-etching of the silicon is performed after deposition and patterning of the metallization. The sensor membrane underneath the meandering resistors has a thickness of 50 µm. The dimensions of the chips is 4 mm × 4 mm. The quadratic membrane has an edge length of 1 mm.

In parallel, we fabricated chips with arrays of platinum µ-strain gauges on the surface. Fig. 1 depicts the pressure sensor design and the layout for the µ-strain gauges. The membrane and cavity sizes are the same for both layouts.

Before assembly, a tempering step of 30 min at 800°C in air was performed.

For the electrical interconnection of the sensors, platinum wire bonding has been approved and can be conducted after the die-attach process [5].

B. Sensor Package and FE Model

In recent publications we presented assembly and interconnection technologies for MEMS operating up to 500°C [6]. The test technologies were rated with regard to stability and stress induced into the sensor. A borosilicate glass solder die-attachment in combination with Si_3N_4 and AlN substrates showed the highest stability after high temperature performance. In Fig. 2, a pressure sensor on AlN and a strain gauge test chip on Si_3N_4 are shown.

The glass soldering was done at 700°C in an argon atmosphere. Fig. 3 depicts a cross section of the sensor element mounted with 40 µm thick layer of glass-solder on a Si_3N_4 substrate.

The thermomechanical simulations were performed with ANSYS Workbench V.14.5. We built a 3D FE model of the different assemblies to simulate the cooling of the device from processing to room temperature. The in-plane stress and out-of-plane chip deformation were obtained from the simulations. Fig. 4 exhibits the 3D element mesh, a quarter model of the pressure sensor.

In Table I, the temperature-dependent material properties are listed that were utilized in the FE simulations. The presented values are predominantly given by the manufacturers of the ceramics and from the literature [7]. Young's modulus E for the glass solder was measured by dynamic mechanical analysis

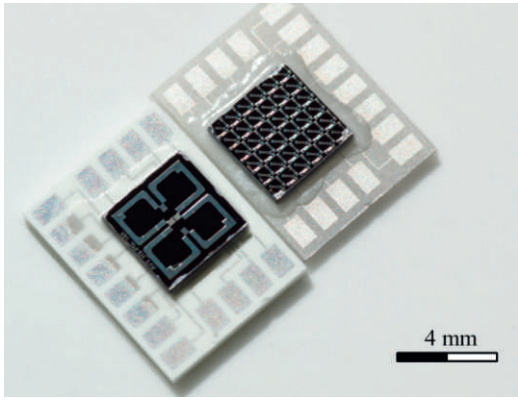

Fig. 2. Micrograph of (left) an assembled pressure sensor on AlN and (right) a µ-strain gauge test-chip on Si_3N_4.

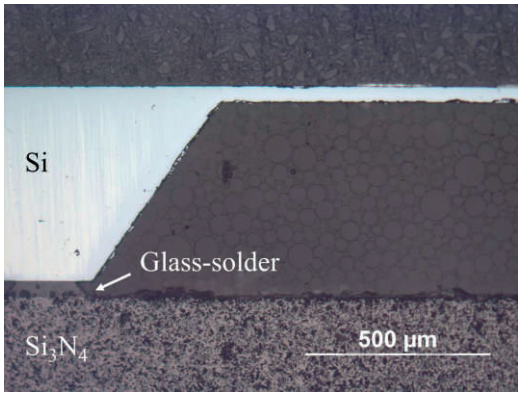

Fig. 3. Micrograph of a cross section through the center of the sensor membrane of an assembly on Si_3N_4.

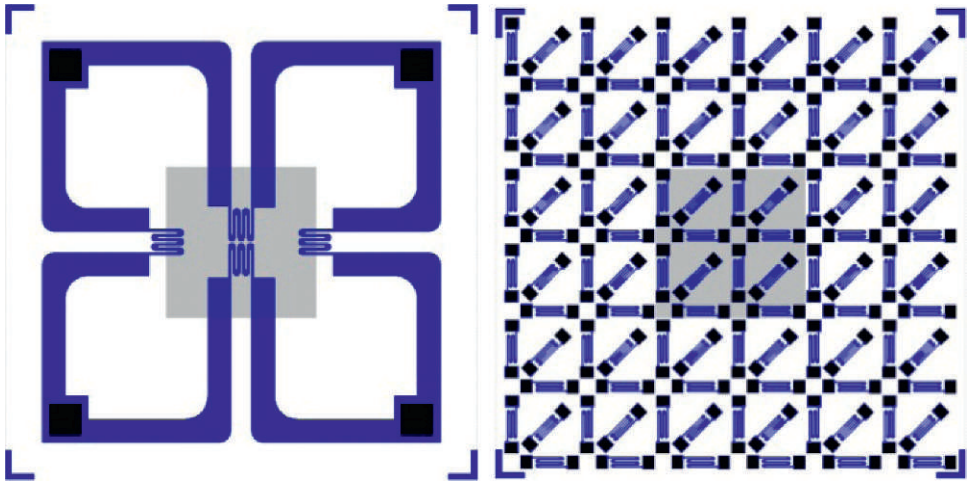

Fig. 1. Sensor design: (left) resistor-bridge for the pressure sensor and (right) layout of the µ-strain gauge test-chip where the gray area indicates the membrane.

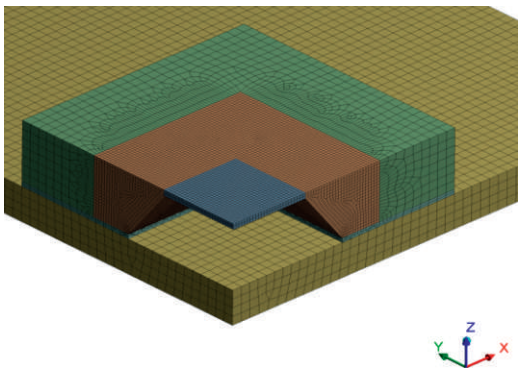

Fig. 4. Meshed FE quarter model of the pressure sensor.

Table I
Material Properties Utilized for the FE Modeling of the Sensor, Die-Attachment, and Substrate [7]

Material property	Temperature range [°C]	Si	AlN	Si_3N_4	Glass solder*
	20-200	2.6	5.2	3	3.6
	200-400	3	6.3	3.05	5.3
α [ppm/K]	400-600	3.2	7.3	3.1	6.7
	20-200	161	310	315	38
	200-400	140	290	312	37
E [GPa]	400-600	120	270	310	32

*Borosilicate.

(DMA) up to 350°C and the coefficient of thermal expansion (CTE) α was measured with thermal mechanical analysis (TMA) up to 600°C.

A linear elastic material behavior with temperature-dependent Young's modulus and CTE was assumed for the ceramic substrates, the glass solder, and the silicon up to 600°C.

Experimental Procedure

A. Strain and Deformation Measurement with Digital Image Correlation

Digital image correlation (DIC) is an approved technology for 3D deformation measurements of electronic devices [8]. We developed a vacuum chamber with an integrated heating stage with a minimum of induced rigid body movement. In a vacuum, disturbed air turbulence caused by temperature differences are mostly eliminated.

The developed setup in combination with a DIC system of the company GOM enables 3D deformation and strain measurements up to 600°C. The test specimen sizes were in the mm-range and were measured with a resolution for deformations of about 1 μm. Within this resolution, the repeatability of the optical measurement is given. Si wafers with platinum-based resistors were diced into strips. We used a tensile testing machine (Z 2010, Zwick Co) to measure the tensile strength of a test strip, interconnected with Pt bonds and glued to metallic holders. Fig. 5 depicts the experimental setup with the DIC-camera system placed in front of the test strip.

Due to a mismatch of the CTEs, thermomechanical stresses are induced in the sensor chip after cooling down from processing temperature. In this case, stress leads to a chip deformation after die attachment, which results in chip warpage.

The chip's warpage at room temperature and the deformation due to increasing temperature can indicate the state of stress in the chip surface where the sensor structures are located. The measured warpage was compared with FEM simulations to validate the model and material parameters that were used. Fig. 6 exhibits the DIC system in combination with the introduced vacuum chamber setup.

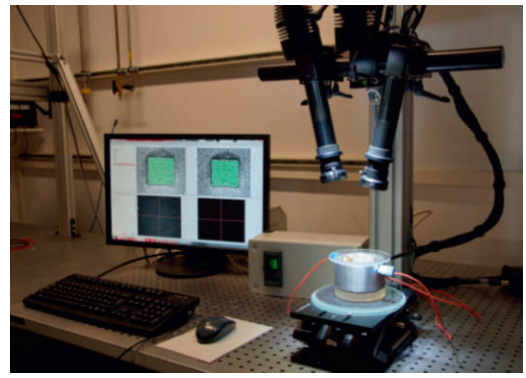

Fig. 6. Setup for DIC measurements with vacuum chamber, temperature controller, and cameras.

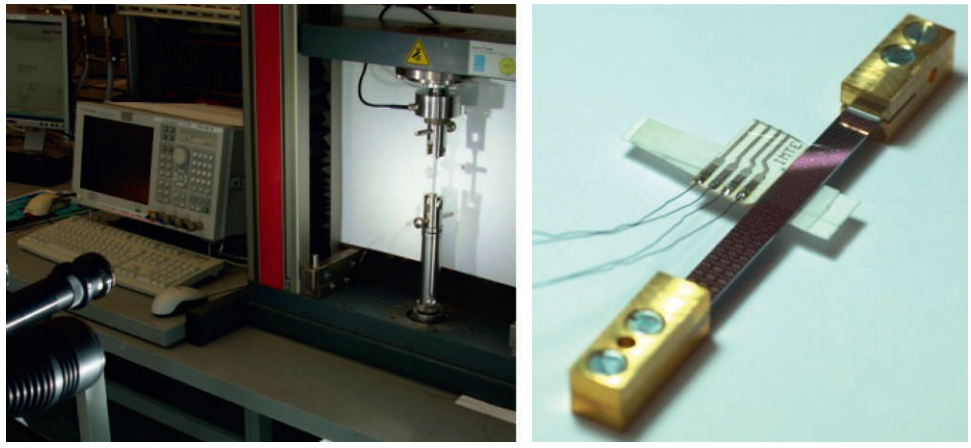

Fig. 5. (Left) Tensile testing machine with specimen and DIC camera system and (right) Si strip with bonds and wiring board for strain gauge characterization.

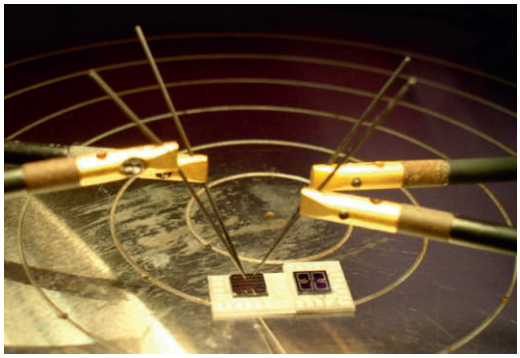

Fig. 7. Test chips during four-probe measurement of the sensor bridge voltage and strain gauge characterization.

The chip deformation of glass soldered sensors was measured from room temperature to 500°C.

B. Sensor and Test Chip Characterization

The analysis of stresses with high temperature stable μ-strain gauges is described in this section. The strains in the surface can be obtained by measuring the change of the resistance after the packaging process applying the gauge factor of the resistive structures. We characterized the introduced Pt-based meanders directly after fabrication and again after the packaging process. A four-probe station from Karl Suss with μ-tips, in combination with digital multimeters from Agilent was used for resistance measurements inside a clean room. Fig. 7 shows two assembled sensors on AlN substrates which were characterized after the glass soldering.

Results and Discussion

A. Gauge Factor of the Platinum Thin Film

For the application of μ-strain gauges it is necessary to identify the strain sensitivity of the utilized thin films. The gauge factor of the investigated platinum gauges was calculated with eq. (1). The strain ε was directly obtained from the optical DIC measurements of the silicon strip with the strain gauges presented in Experimental Procedure section A. Fig. 8 exhibits the results for the strain gauge resistance as a function

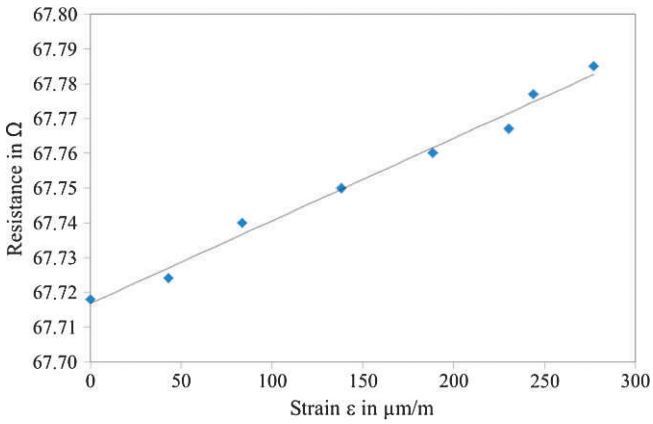

Fig. 8. Resistance of the μ-strain gauges as a function of optically measured strain in the Si-strip at 25°C.

Table II
Results for the Sensor Bridge Voltages and Strain Gauge Resistances at Room Temperature

Assembly	Bridge voltage [mV/V]	μ-Strain gauges [Ω]
Bare chip	25.4	34.97
Chip on AlN	35.4	33.24
Chip on Si_3N_4	34.1	34.76

of strain, measured at room temperature. The gauge factor was GF = 3.57. This value is in good agreement with earlier published results for 1 μm thick platinum thin films [9].

B. Strain Gauges and Bridge Voltage Measurements

The bridge voltage of the pressure sensors and the resistance of the μ-strain gauges were measured. Here bare chips which had the same temperature treatment as the glass-soldered sensors were distinguished from the devices mounted on AlN and on Si_3N_4 substrates. At least three specimens out of each group were measured and the average value was calculated. In Table II the results of the electrical characterization are summarized.

The bridge voltage increased by 40% from 25.4 mV/V for bare chips to 35.4 mV/V for sensors on AlN. For devices on Si_3N_4, the bridge signal increase was 34% from the initial 25.4 mV/V to 34.1 mV/V.

Given a multimeter accuracy of 0.014% for resistance measurements and eq. (1), a detectability limit and resolution of $\Delta\varepsilon = 40$ ppm can be calculated for the strain gauges with the gauge factor k of GF = 3.57. Above this lower limit, the repeatability of the measurements is ensured.

The resistance of the strain gauges on top of the membrane decreased in average by 1.73 Ω (5%) for test chips on AlN and by 0.21 Ω (0.6%) for strain gauges on Si_3N_4. By the determined gauge factor GF = 3.57, it was possible to make an estimation about the strain in the test chip membrane. For devices on AlN a value of $\varepsilon_{AlN} = -1.39\%$ was calculated. The strain in the membrane for devices on Si_3N_4 was determined as $\varepsilon_{Si3N4} = -0.168\%$. The simulation result for average in-plane stresses for the sensor membrane was −45 MPa for devices on AlN. A higher stress gradient was found for the AlN assemblies compared with Si_3N_4 assemblies. The higher drift of the bridge voltage after the assembly process, shown in Table II, can be explained by a higher stress gradient in the membrane.

C. Chip Deformation over Temperature: DIC versus FEM

The out-of-plane deformation in the z axis was measured with DIC over temperatures up to 500°C for the assembled pressure sensors. Fig. 9 exhibits a contour plot of (left) the measured absolute z coordinate and (right) the deformation Δz for an assembly with AlN substrate, presenting path x along the chip's diagonal. The sensor warpage is convex with a maximum deflection of 4.5 μm.

Fig. 10 depicts FEM results for the chip surface out-of-plane deformation after cooling down from the glass transition temperature $T_g = 550$°C of the glass solder. The maximum deflection of the chip was 5 μm. In Fig. 11 the results for the DIC

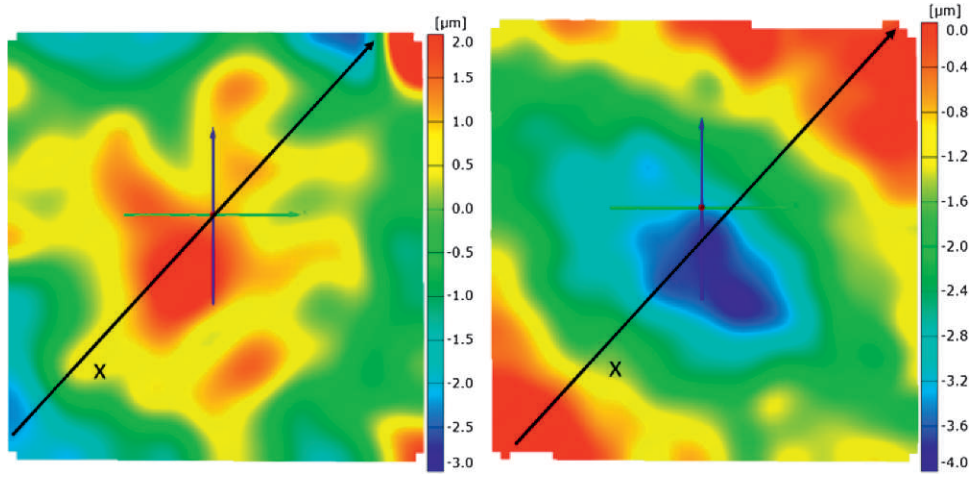

Fig. 9. DIC measurement sensor on AlN: (left) z coordinate contours at 25°C, chip deflection: 4.9 µm, (right) contours of Δz from 25-500°C of sensor surface.

measurements on path x and the FE simulation results for AlN devices are shown.

The deviation between measurement and simulation was 0.3 µm and thus 6% of the measured deformation. For sensors on Si_3N_4, the deviation is 15%. The higher deviation value can be explained by the minor variations of the materials data used for Si_3N_4. Fig. 12 exhibits experimental results compared with FE simulation data of the out-of-plane coordinate z and the deformation Δz on path x.

The optical measurement verified the FE model for both assemblies with a low deviation.

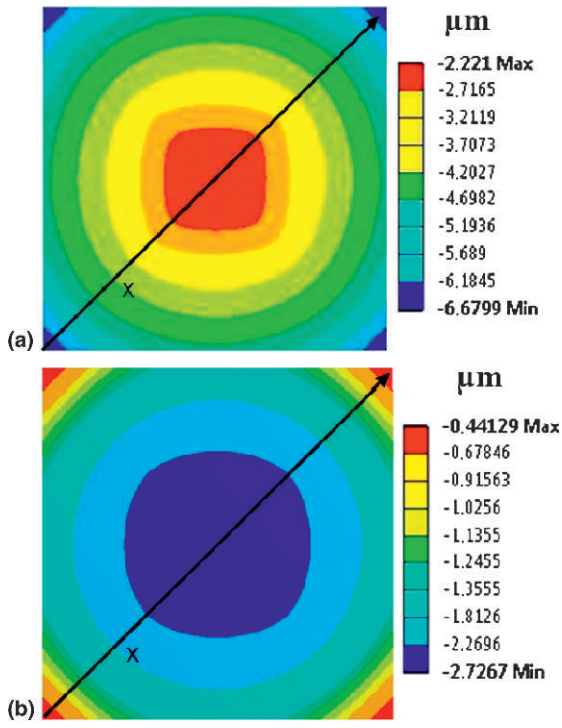

Fig. 10. FEM simulation of glass soldered assemblies: (a) AlN substrate: z coordinate contours of the chip deformation at 25°C, chip deflection: 4.4 µm. (b) Si_3N_4 substrate: z-coordinate contours of the chip at 25°C, chip deflection: −3 µm.

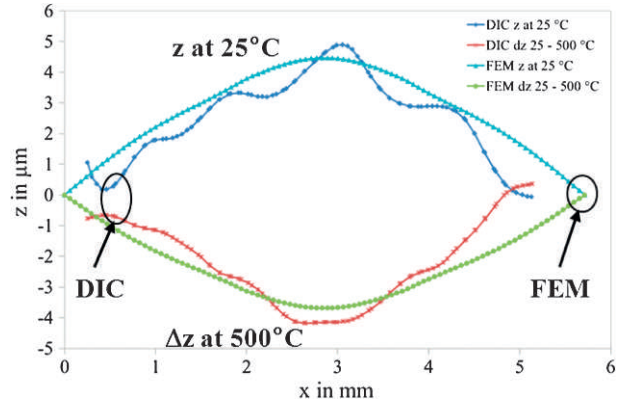

Fig. 11. DIC versus FEM: z coordinate of sensor surface mounted on AlN substrate at 25°C and deformation Δz of sensor surface from 25-500°C.

D. Stress Induced by the Assembly Process

The stress in the chip surface obtained from the measurements of the µ-strain gauges and the values received from FEM indicated high compressive stresses in the sensor membrane. This stress is induced by the assembly process and is higher for devices on AlN. Fig. 13 depicts the simulation results for the

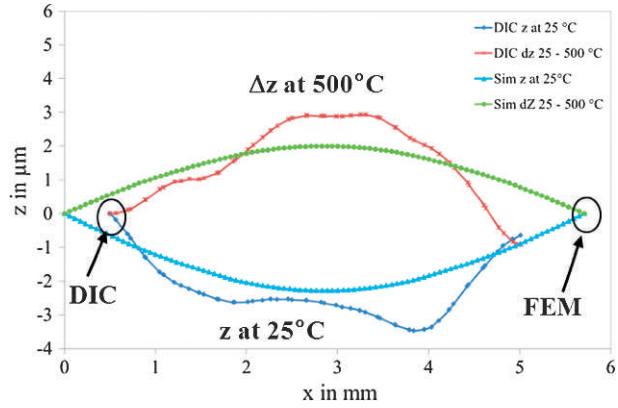

Fig. 12. DIC versus FEM: z coordinate of the sensor surface mounted on Si_3N_4 substrate at 25°C and deformation Δz of the surface from 25-500°C.

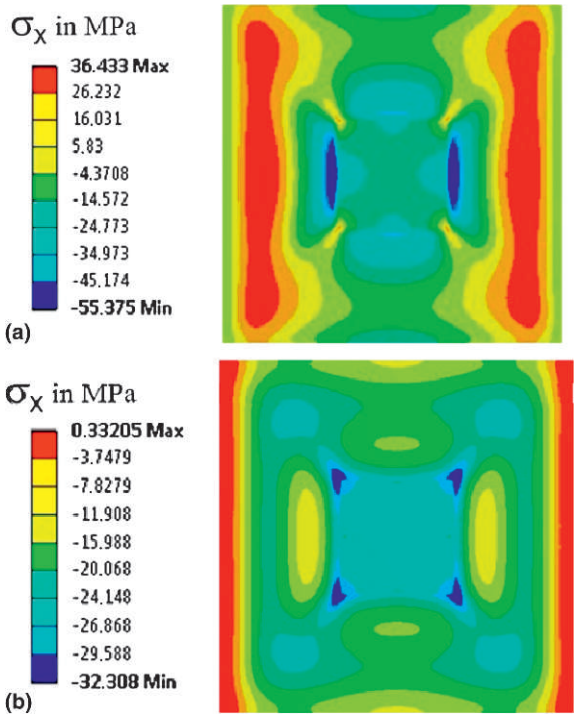

Fig. 13. FEM simulation of sensor chip assembly. Contour plot of in-plane-stress σ_x: (a) AlN substrate, (b) Si_3N_4 substrate.

stress in the chip surface after cooling down to 25°C from T_g for AlN assemblies. The in-plane-stress at the position of the bridge resistors was −45 MPa in the longitudinal direction.

For the assembly with the Si_3N_4 substrate, an in-plane stress of −20 MPa was obtained in the longitudinal direction at the position of the bridge meanders. A higher stress gradient in the membrane at the resistor positions was obtained for AlN assemblies.

Conclusion

High temperature stable assembly technologies induce high mechanical stresses into the sensor element. In this paper, techniques have been presented to analyze the stresses induced by the package and their influence on the sensor output signal. The focus of the paper is on the methodology as well as on the comparison of AlN and Si_3N_4 as sensor substrate. We investigated glass soldering of dice on both ceramic substrates. Pressure sensors with platinum metallization for operation up to 500°C were processed in thin film technology. First, gauge factor measurements with a tensile testing machine in combination with optical strain measurements were performed. They revealed a gauge factor GF = 3.6 for the investigated platinum thin films. With these sensors and thin film strain gauge test chips, the stress state in μ-membranes was investigated. The strain in the chip surface was measured with the μ-strain gauges and revealed a strong dependency on the substrate CTE. For both assemblies, compressive in-plane stresses in the sensor membrane were obtained from the μ-strain gauges and the FEM simulations. Furthermore, the simulations were verified by optical out-of-plane deformation measurements up to 500°C. Higher stresses and chip deflections were found for AlN assemblies, induced by the increased CTE mismatch of substrate and chip. The higher values of compressive stresses in the sensor membrane led to a stronger sensor offset drift for devices on the AlN substrate according to the measurements after the assembly process. The presented results indicate that the Si_3N_4 substrate is more appropriate for the sensor assembly, in terms of induced stress and shifting of the sensor signal.

In further research, novel ceramic substrates with closer matching CTEs to silicon will be investigated regarding their influence on stress in the chip and the sensor signal behavior. The pressure sensors will be further miniaturized and interconnected with high temperature stable flip-chip technologies.

Acknowledgments

The investigations presented in this paper were funded by the German Federal Ministry of Education and Research, BMBF, within the "Spitzencluster" project SiC-Tech, FKZ: 16SV5127. The authors are very grateful for this financial support.

References

[1] N. Behnel, T. Fuchs, and H. Seidel, "New SiC pressure-sensor-technologies for harsh environments," Proceedings of Mikrosystemtechnik Kongress, Berlin, October 2009.

[2] A.A. Ned, R.S. Okojie, A.D. Kurtz, and W.H. Ko, "6H-SiC pressure sensor operation at 600°C," Proceedings of the High Temperature Electronics Conference, pp. 257-260, 1998.

[3] P. Hagler, P. Henson, and R.W. Johnson, "Packaging technology for electronic applications in harsh high-temperature environments," *IEEE Transactions on Industrial Electronics*, Vol. 58, No. 7, pp. 2673-2682, 2011.

[4] P.P.L. Regtien, *Sensors for Mechatronics*, Elsevier, London, pp. 68-69, 2012.

[5] R. Zeiser, P. Wagner, and J. Wilde, "Investigation of ultrasonic platinum and palladium wire bonding as interconnection technology for high-temperature SiC-MEMS," Proceedings of the IEEE Electronics System Integration Technologies Conference, Amsterdam, September, pp. 1-6, 2012.

[6] R. Zeiser, P. Wagner, and J. Wilde, "Assembly and packaging technologies for high-temperature SiC sensors," Proceedings of the 62nd Electronic Components and Technology Conference, San Diego, CA, June, pp. 338-343, 2012.

[7] L. Coppola, D. Huff, F. Wang, R. Burgos, and D. Boroyevich, "Survey on high-temperature packaging materials for SiC-based power electronics modules," Proceedings of the Power Electronics Specialists Conference, pp. 2234-2240, 2007.

[8] P. Lall, D. Panchagade, D. Iyengar, S. Shantaram, J. Suhling, and H. Schrier, "High speed digital image correlation for transient-shock reliability of area-array packages," Proceedings of the 57th Electronic Components and Technology Conference, Reno, NV, June, pp. 924-939, 2007.

[9] S. Fricke, A. Friedberger, G. Mueller, H. Seidel, and U. Schmid, "Strain gauge factor and TCR of sputter deposited Pt thin films up to 850°C," Proceedings of the IEEE Sensors Conference, Lecce, Italy, October, pp. 1532-1535, 2008.